

Current problems in semiconductor detectors for HEP after particle irradiation

Ionel Lazanu

University of Bucharest, Department of Nuclear Physics

POBox MG-11, Bucharest – Magurele, Romania

e-mail: Ionel.Lazanu@fpca2.fizica.unibuc.ro

(Received September 25, 2002)

The use of semiconductor materials as detectors in high radiation environments, as to be expected in future high energy accelerators or in space missions, poses severe problems in long-time operations, due to changes in the properties of the material, and consequently in the performances of detectors.

This talk presents the major theoretical areas of current problems, and reviews the works in this field and the stage of their understanding, including author's contributions.

The mechanisms of interaction of the projectile with the semiconductor, the production of primary defects, the physical quantities and the equations able to characterise and describe the radiation effects, the equations of kinetics of defects are considered. Correlation between microscopic damage and detector performances and the possible ways to optimise the radiation hardness of materials are discussed.

Keywords: semiconductor detectors, radiation bulk damage, hadrons, kinetics of defects, detector characteristics.

1. Introduction

Semiconductor based devices are widely used in a variety of application fields, characterised by hostile radiation environments. For this reason, radiation-damage research has been extensively developed in the past in view to assess the radiation-induced performance degradation of detectors and devices to be used in high energy physics, space missions, in military, industrial and medical applications or radiation dosimetry.

A strong effort was spent in particular to correlate the changes in the electrical properties of irradiated detectors and devices with radiation-induced lattice defects. These studies permit to progress in both fundamental research and technological development.

This talk attempts to discuss the current knowledge of radiation damage in semiconductor materials for HEP environment applications and to summarise the main author's results in this field, particularly for silicon. The analysis is concentrated on the most important features from the point of view of basic research studies.

Energetic particles passing through matter lose energy through a variety of interaction mechanisms.

Two major consequences result from the energy transfer from the incident projectile to the semiconductor material, namely ionisation and atomic displacement. Ionisation (effect of the projectile particle with the atomic electrons) is the phenomenon used in the detection, while atomic displacements (produced by the interaction between the incident particle with the atomic target) induce generally serious degradation effects in the intrinsic material properties, which are observed in the modifications of device parameters. These are the principal obstacles to long-term operation of semiconductor detectors and devices in intense field of radiation as those in the high energy physics at the particle colliders or in space missions.

In the primary interactions between energetic radiation and the electronic structure of atoms - despite the initial variety of interactions - much of this loss of energy is ultimately converted to the form of electron-hole pairs. In this process, known as ionisation, the valence band electrons in the solid are excited to the conduction band and are highly mobile if an electric field is applied. In

principle, this phenomenon is used in detection, the concrete realisation been different for different semiconductors.

Ionisation can produce also a large variety of phenomena in materials or in devices, but will not be discussed in this talk.

A special case of ionisation effects is the single-event phenomenon, which covers both single-event upset (SEU) or soft error, and latch-up. Cosmic rays are considered as main sources for these events, but, in some conditions, the recoil nuclei obtained from atomic displacements could also generate this effect.

The consequences of ionisation processes are not considered here and only the bulk effects are discussed in detail.

2. Production of primary defects

When a momentum exchange occurs between a high energy particle and an atom in a solid, the target atom is likely to leave its position at high velocity and is known as the "knock-on". The atom will leave its site if it receives an amount of energy greater than the displacement energy, E_d . The atomic displacement processes are conventionally known as "bulk damage".

2.1 Mechanisms of interaction

The mechanism considered in the study of the interaction between the incoming particle and the solid, by which bulk defects are produced, is the following: the particle, with electrical charge or not, interacts with the nuclei of the crystalline lattice. As a result of the interaction, depending on the energy and on the nature of the incident particle, one or more light particles are produced, and usually one or more heavy recoil nuclei. These nuclei have charge and mass numbers lower or at least equal with those of the medium. After the interaction process, the recoil nucleus or nuclei, if they have sufficient energy, are displaced from the lattice positions into interstitials. Then, the primary knock-on nucleus, if its energy is large enough, can produce the displacement of a new nucleus, and the process could continue as a cascade, until the energy of the nucleus becomes lower than the threshold for atomic displacements. Because of the regular nature of the crystalline lattice, the displacement energy is anisotropic. Because the multitude of inelastic channels, in the concrete evaluation of defect production, the nuclear interactions must be modelled in some simplifying hypothesis.

2.2 Physical quantities that characterise the radiation effects in semiconductor materials

There is not one physical quantity dedicated to the global characterisation of the effects of radiation in the semiconductor material.

Historically, the NIEL (Non Ionising Energy Loss) was used in relation with induced defects in material. For practical reasons, has decided to use the 1 *MeV* neutron irradiation as a reference and to refer to other irradiation conditions as relative values. This point of view causes some problems. First, there exist some controversies about the NIEL value induced by 1 *MeV* neutrons. The second argument - this represents a conceptual difficulty, and is discussed below.

Another possible one - proposed by the author [1] to characterise these effects is the concentration of primary radiation induced defects per unit particle fluence (CPD). This last physical quantity has some advantages over NIEL. Because the important weight of annealing processes of primary defects in semiconductors, generally, CPD is not a measurable physical quantity.

The concentration of the primary radiation induced defects per unit fluence in the binary compound *XY*, for example, can be calculated using the explicit formula:

$$CPD(E) = \sum_m \frac{N_m}{2E_{d;m}} \int \sum_i \left(\frac{d\sigma}{d\Omega} \right)_{i;m} L(E_{Ri})_{XY} d\Omega = \frac{1}{N_A} \sum_m \frac{N_m A_m}{2E_{d;m}} (NIEL)_{XY}^{m_family} \quad (1)$$

$m = X, Y$

where E is the kinetic energy of the incident particle, N_m is the atomic density of the $X(Y)$ in XY compound, A_m is the atomic number of the $X(Y)$, $E_{d;X(Y)}$ - the threshold energy for displacements in the $X(Y)$ sublattice of the XY compound, E_{Ri} - the recoil energy of the residual nucleus produced in interaction i , $L(E_{Ri})$ - the Lindhard factor that describes the partition of the recoil energy between ionisation and displacements and $\left(\frac{d\sigma}{d\Omega} \right)_i$ - the differential cross section of the interaction between the incident particle and the nucleus of the lattice for the process or mechanism (i), responsible in defect production.

The atomic density in the XY compound is a material parameter. The formula gives also the relation with the non ionising energy loss . N_A is Avogadro's number. It is important to observe that there exists a proportionality between the CPD and NIEL only for monoelement materials, and this proportionality can be extended only approximately for compounds with neighbouring elements in the periodic table, e.g. for GaAs.

The CPD allows the comparison of the effects produced by the same particle in different materials, while NIEL can be used especially for the comparison of the effects produced in the same material by different particles.

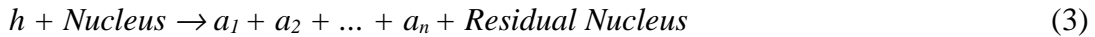
2.3 Modelling of the mechanisms of interaction

The contribution of each channel to the total concentration of defects depends on the probability of interaction and on the kinematics of the process, reflected in the recoil energy of the residual nucleus. For example, if the incident particle is a hadron, in an elastic scattering process of interaction, symbolically represented by:



the hadron does not excite the target nucleus.

The inelastic hadron - nucleus scattering includes all reactions of the type:



where the reaction products a_1, a_2, \dots, a_n can be pion, proton, neutron, deuteron, other particles or light nuclei.

When the kinetic energy of the incident particle exceeds the threshold energy of 140 MeV, secondary pions could also be produced.

If the inelastic process is produced by nucleons, the identity of the incoming projectile is lost, and the creation of the secondary particles is associated with energy exchanges which are of the order of MeV or larger.

The interaction of pions with nuclei at low and medium energies, i.e. for pion kinetic energies below 300 MeV, presents two specific phenomena: the absorption of pions by the nucleus (the process by which the pion disappear as a real particle) and the production of the delta resonance in the nucleus. The pion deposits at least 140 MeV in the nucleus and the pion interaction with two nucleons is the simplest mechanism by which a pion can be absorbed. The delta resonance (1232

MeV in mass), with a width of about 100 MeV, dominates the pion-nucleon scattering between 100 and 300 MeV pion kinetic energy. The delta resonance is produced and experimentally observed also in the pion-nucleus interaction, so a large peak dominates the region between 100 and 300 MeV in all interaction channels; no clear structure is observed at higher energies.

At energies above 500 MeV, the particular features of the pion become less important, and pion-nucleus interaction does not differ significantly from the scattering of any other high energetic hadron by nuclei. Pions with energies of the order of hundreds of MeV, which are scattered by silicon, produce defects in the silicon lattice structure by four mechanisms: Rutherford, nuclear elastic, inelastic scattering and absorption. While the first three processes are characteristic also to protons, the last one is specific to the pion-nucleus interaction.

For nuclei with $Z=N=A/2$, the Coulomb potential modifies the π^+ and π^- nucleus cross sections in two physically different ways [2]: (i) the π^- is accelerated and the π^+ slowed down, when they approach the nucleus, having this way different kinetic energies at the nuclear surface; this leads to $\sigma_{\pi^-A} > \sigma_{\pi^+A}$ below the peak and $\sigma_{\pi^+A} > \sigma_{\pi^-A}$ above. (ii) The pion trajectories outside the nucleus are not straight lines, but the π^- are attracted and the π^+ repelled, this argument leading to higher π^- - nucleus cross sections. The differences between π^- and π^+ -nucleus cross sections become less important at high energies, far from the resonance, where the weight of the Coulomb interaction decreases.

Rutherford and nuclear elastic scattering of charged hadrons on nuclei cannot be treated separately due to strong interference mechanisms [3-4]. In the energy range of the delta resonance, for pion interactions, the total inelastic cross section is of the same order of magnitude as the elastic one, and remains approximately constant outside this region, at higher energies, becoming large relatively to elastic processes.

For the inelastic processes, there is a multitude of open channels, corresponding to possible final states. In order to obtain an estimate of the average recoil energies, some simplifying assumptions concerning the inelastic interactions have to be made, starting from the available experimental data. The much deeper investigation of the resonance region, as well as its greater importance for the radiation damage phenomena led us to study this energy range separately. The inelastic interaction has been supposed to be composed from the knock-out of one nucleon, and a rest given by a multiple interaction background, on an effective number of nucleons that are removed from the nucleus. The weight of the knock-out from the total inelastic has been estimated considering this process as the sum of the knock-out of one proton and one neutron, using the data from [5-8]. The effective number of nucleons has been extracted from the literature in the region of the delta resonance [9], and have been evaluated at higher energies considering the pion nucleon cross sections. To calculate the energy of the recoil, the momenta of the outgoing hadrons have been supposed to compensate each other. The multifragmentation process, as well as particle production, have been neglected.

The pion absorption has no correspondent to the more studied cases of proton and neutron interaction with silicon. Some simplifying considerations was supposed. The mechanism of absorption on a nucleon pair was demonstrated to be independent on the mass number A [10]. So, the absorption on a nucleon pair could be considered to have equal weights in silicon as in other nuclei. We have chosen carbon [11], that has the same Z/A as silicon. The nucleons have been supposed to be emitted preponderantly at 180° , in agreement with [12]. The remaining part of the absorption has been attributed to the simultaneous absorption on more nucleons. We supposed a simultaneous absorption on an effective number of nucleons [6]. In order to attribute weights to the absorption on an effective number of nucleons, we supposed that the probability of pion absorption on n nucleons is a decreasing function, having an exponential slope that has been determined from experimental data [13-14]. The nucleons have been supposed to be emitted isotropically.

In the energy range of interest for the present calculations, the inelastic cross-section is of the same order of magnitude as the elastic one. The inelastic interaction has been supposed to be composed from the knock-out mechanism and all other channels have been considered as equivalent to the interaction on an effective number of nucleons. The energy dependence of the weight of the knock-out has been estimated using the data from [5-6, 9]. The interaction on an effective number of nucleons has been considered equivalent to the fragmentation into two nuclei, the first of mass number n_{eff} , and the other of mass number $(A-n_{\text{eff}})$. The energy dependence of the effective number n_{eff} has been determined by Ashery et.al. [9] from the experimental data, and has been used in the present work.

2.4 Analytical approximations of the equations describing radiation effects

Two different models have been developed to evaluate the partition of the energy of the incoming particle between ionisation and displacements: the model of Kinchin and Pease [15] and Lindhard theory [16].

In HEP, the most used is the Lindhard theory.. In the paper [17] the original Lindhard's theory was extended, using analytical approximations, to one side to the case of the incident ions is different to the target ones and the other side to the case of compound (multi-element) materials.

A similar generalisation, but using Monte Carlo simulations was developed by the T. Sloan and co-workers [18].

For a given medium, consisting of only one atomic species, the family of curves characterising the dependence of the energy channelled into displacements, as a function of the recoils energy, and having the mass and charge numbers ($Z_{\text{part}} \leq Z_{\text{med}}$ and $A_{\text{part}} \leq A_{\text{med}}$) as parameters, has the following characteristics:

- The maximum energy transferred into displacements corresponds to particles identical to the medium ones.
- All curves start, at low energies, from the same curve; they have at low energies identical values of the energy spent in displacements, independent on the charge and mass number of the recoil, and, roughly, an $E^{0.9}$ dependence.
- At higher energies, the curves start to detach from this main branch. This happens at lower energies if their charge and mass numbers are smaller. Then, the curves present a smooth increase with the energy. This means that at high enough energy of the incident particle, the increase of its energy determines, mainly, an increase of the ionisation loss. The asymptotic limit (E_p) of the equation (6) depends on the characteristics of the particle and of the medium as:

$$\frac{\left(Z_{\text{part}}^{2/3} + Z_{\text{med}}^{2/3} \right)^2}{Z_{\text{part}}^{1/3}} \cdot \frac{A_{\text{part}}^3}{\left(A_{\text{part}} + A_{\text{med}} \right)^2} \quad (4)$$

In the particular case of a particle belonging to the medium, the value of this energy is proportional to the product of the mass and charge numbers; if, more, $Z \approx A/2$, as is the case of C in diamond, Si in silicon and Ge in germanium, an $A^{\approx 2}$ dependence is obtained for E_p .

In fact, the solution given by equation (6) is the most important in the evaluation of the bulk damage produced in materials, in accelerator applications.

The case of **binary media** has been treated, in a first approximation, as specified before, considering separately the two components, and then weighting with their number in the molecule.

If the two components are adjoining each other in the periodic table, as is the case of, e.g., GaAs and InSb, then there is no significant difference in the Lindhard partition energy curves, for element placed between the two elements of the compound.

If the two components are far from each other in the periodic table, then there are, in principle, two families of curves, one corresponding to the heaviest element, the other to the lightest one, separated by a gap.

In Figure 1 the energy dependence of CPD in silicon produced by pions, protons, neutrons, electrons and photons are presented. For pions the calculations from reference [19] have been used; for protons and electrons, the results of Summers and of van Ginneken have been used [20, 21]. The curves for photons and neutrons are calculated by van Ginneken [21] and Ougoung [22] respectively.

3. The present understanding of the radiation-induced lattice disorder

3.1 Defects induced after irradiation

There is a wide literature discussing the problem of defect introduction by irradiation in silicon, starting in the 50's and widely spreading in time up to now days. A wide review of this subject can be found e.g. in [23, 24].

A collection of the most important deep-defects observed in silicon is presented in Table 1.

Table 1: Irradiation defects in silicon

| Defect identity | Charge states | Energy level [eV] |
|-----------------|---------------|--------------------------|
| V_2O | | $E_C - (0.5 \div 0.54)$ |
| Si_i | | $E_C - 0.49$ |
| VP | | $E_C - (0.4 \div 0.46)$ |
| V_2 | V_2^0 | $E_C - (0.39 \div 0.41)$ |
| | V_2^+ | $E_C - (0.23 \div 0.25)$ |
| | V_2^- | $E_V + (0.21 \div 0.25)$ |
| C_iO_i | | $E_V + (0.36 \div 0.38)$ |
| C_i | | $E_V + (0.3 \div 0.33)$ |
| VO | VO^- | $E_C - 0.17$ |
| | VO^0 | |
| C_iC_s | | $E_V + 0.17$ |

Defects as phosphorus-vacancy, vacancy-oxygen, divacancy in different charge states and carbon-related traps as interstitial carbon C_i or complexes as C_iC_s or C_iO_i have been intensively

studied in past. Midgap defects, characterised by energy levels at ≈ 0.5 eV from the valence or conduction band edges have been detected quite more recently.

Also, a vast literature is dedicated to cluster of lattice defects. The cluster defects are considered as responsible for the main damage in silicon, but the experimental evidence is confused, consequence their parameters are contradictories.

3.2 The kinetics of radiation induced defects

Silicon used in high-energy physics detectors is n-type high resistivity ($1 \div 6$ K Ω cm) phosphorus doped FZ material.

The effect of oxygen in irradiated silicon has been a subject of intensive studies in remote past. In the last decade, a lot of studies have been performed to investigate the influence of different impurities, especially oxygen and carbon, as possible ways to enhance the radiation hardness of silicon for detectors in the future generation of experiments in high energy physics - see, e.g. references [25, 26]. Some people consider that these impurities added to the silicon bulk modify the formation of electrically active defects, thus controlling the macroscopic device parameters. Empirically, it is considered that if the silicon is enriched in oxygen, the capture of radiation-generated vacancies is favoured by the production of the pseudo-acceptor complex vacancy-oxygen. Interstitial oxygen acts as a sink for vacancies, thus reducing the probability of formation of the divacancy related complexes, associated with deeper levels inside the gap.

The concentrations of interstitial oxygen O_i and substitutional carbon C_s in silicon are strongly dependent on the growth technique. In high purity Float Zone Si, oxygen interstitial concentrations are around 10^{15} cm^{-3} , while in Czochralski Si these concentrations can reach values as high as 10^{18} cm^{-3} . Because Czochralski silicon is not available in detector grade quality, an oxygenation technique developed at BNL produces Diffusion Oxygenated Float Zone in silicon, obtaining a O_i concentration of the order 5×10^{17} cm^{-3} . These materials can be enriched in substitutional carbon up to $[C_s] \approx 1.8 \times 10^{16}$ cm^{-3} .

After the irradiation of silicon, the following stable defects have been identified (see References [23, 24]): Si_i , VP , VO , V_2 , V_2O , C_iO_i , C_i , C_iC_s .

The pre-existing thermal defects and those produced by irradiation, as well as the impurities, are assumed to be randomly distributed in the solid. An important part of the vacancies and interstitials annihilate. The sample contains certain concentrations of impurities, which can trap interstitials and vacancies respectively, and form stable defects.

Vacancy-interstitial annihilation, interstitial migration to sinks, divacancy, vacancy and interstitial impurity complex formation are considered. The role of phosphorus, oxygen and carbon is taken into account, and the following stable defects : VP , VO , V_2 , V_2O , C_i , C_iO_i , C_iC_s , are considered. Other possible defects as V_3O , V_2O_2 , V_3O_3 [27], are not included in the present model.

The following picture describes in terms of chemical reactions the mechanisms of production and evolution of the defects considered in the present paper:



(VO is the A centre).



(VP is the E centre).



Some considerations about the determination of the reaction constants are given in references [28, 29].

The reaction constants K_i ($i = 1, 3 \div 10$) have the general form:

$$K_i = C \cdot \nu \cdot \exp(-E_i / k_B T) \quad (15)$$

with ν the vibration frequency of the lattice, E_i the associated activation energy and C a numerical constant that accounts for the symmetry of the defect in the lattice.

The reaction constant related to the migration of interstitials to sinks could be expressed as:

$$K_2 = \alpha \cdot \nu \cdot \lambda^2 \exp(-E_2 / k_B T) \quad (16)$$

with α : the sink concentration and λ the jump distance.

The system of coupled differential equations corresponding to the reaction scheme (5) ÷ (14) cannot be solved analytically and a numerical procedure was used.

The following values of the parameters have been used: $E_1 = E_2 = 0.4$ eV, $E_3 = 0.8$ eV, $E_4 = 1.4$ eV, $E_5 = 1.1$ eV, $E_6 = 1.3$ eV, $E_7 = 1.6$ eV, $E_8 = 1.3$ eV, $E_9 = 1.7$ eV, $\nu = 10^{13}$ Hz, $\lambda = 10^{15}$ cm², $\alpha = 10^{10}$ cm⁻².

3.3 Rates for production of defects

The basic assumption of the present model is that the primary defects, vacancies and interstitials, are produced in equal quantities and are uniformly distributed in the material bulk. They are produced by the incoming particle, as a consequence of the subsequent collisions of the primary recoil in the lattice, or thermally (only Frenkel pairs are considered). The generation term (G) is the sum of two components:

$$G = G_R + G_T \quad (17)$$

where G_R accounts for the generation by irradiation, and G_T for thermal generation.

In the simplifying hypothesis of random distribution of CPD for all particles, the identity of the particle is lost after the primary interaction, and two different particles could produce the same generation rate (G_R) for vacancy-interstitial pairs if the following condition:

$$G_R = [(CPD)_{part.a}(E_1)] \times \Phi_{part.a}(E_1) = [(CPD)_{part.b}(E_2)] \times \Phi_{part.b}(E_2) \quad (18)$$

is fulfilled. Here, Φ is the flux of particles of type a and b respectively, and E_1 and E_2 their corresponding kinetic energy.

4. Comparison between model prediction and experimental results

The model predictions have been compared with experimental measurements. A difficulty in this comparison is the insufficient information in published papers regarding the characterisation of silicon, and on the irradiation parameters and conditions for most of the data.

It was underlined in the literature [30] that the ratio of VO to VP centres in electron irradiated silicon is proportional to the ratio between the concentrations of oxygen and phosphorus in the sample. For electron irradiation, in Ref. [31] a linear dependence of the V_2 versus VO centre concentration has been found experimentally. In the present paper, the ratio of concentrations of V_2 to VO centres and VO to VP ones has been calculated in the frame of the model, for the material with the characteristics specified in Ref. [31], and irradiated with 12 MeV electrons, in the conditions of the above mentioned article. The time dependence of these two ratios is represented in Figure 2. Annealing is considered both during and after irradiation. It could be seen that for the ratio of V_2 and VO concentrations the curves corresponding to different irradiation fluences are parallel, while the ratio of VO to VP concentrations is fluence independent, in the interval $2 \times 10^{13} \div 5.5 \times 10^{14} \text{ cm}^{-2}$, in good agreement with the experimental evidence. The ratio between V_2 and VO concentrations is determined by the generation of primary defects by irradiation, while the ratio between VO and VP concentrations is determined by the concentrations of oxygen and phosphorus in silicon.

Our estimations are also in agreement with the measurements presented in reference [32], after electron irradiation, where defect concentrations are presented as a function of the time after irradiation. In Figure 3, both measured and calculated dependencies of the VO and VP concentrations are given. The irradiation was performed with 2.5 MeV electrons, up to a fluence of $3 \cdot 10^{16} \text{ cm}^{-2}$. A good agreement can be observed for these concentrations. The dependencies put in evidence the important role played by the carbon-related defects. The relative values are imposed by the arbitrary units of experimental data.

Also, a good agreement has been obtained between the absolute values of concentrations of $VP + V_2$ and $C_i C_s$ predicted by the model, and the experimental results after 1 MeV neutron irradiation at a total fluence of $5.67 \times 10^{13} \text{ cm}^{-2}$, reported in reference [33]. The calculated $1.5 \cdot 10^{13} \text{ cm}^{-3}$ and $4.1 \cdot 10^{12} \text{ cm}^{-3}$ concentrations for $VP + V_2$ and $C_i C_s$ respectively, are in accord with the values of $1.1 \cdot 10^{13} \text{ cm}^{-3}$ and $3.8 \cdot 10^{12} \text{ cm}^{-3}$, measured experimentally. For the VO concentration, a poorer concordance has been obtained.

5. The influence of initial impurities and irradiation conditions on defect production and annealing in silicon and in particle detectors

5.1 In the semiconductor material

The formation and time evolution of stable defects depends on various factors, e.g. the concentrations of impurities pre-existent in the sample, the rate of generation, the temperature and the history of the irradiation process.

In Figures 4 a) ÷ f), and 5 a) ÷ f) the formation and time evolution of the vacancy-oxygen, vacancy-phosphorus, divacancy, divacancy-oxygen, carbon interstitial - oxygen interstitial and carbon interstitial.- carbon substitutional are modelled in silicon containing different initial concentrations of phosphorus, oxygen and carbon, and for two very different rates of generation.

In Figure 4, the evolution of defect concentrations during high rate irradiation ($G_R = 7 \cdot 10^8 \text{ VI} - \text{pairs}/\text{cm}^3 \text{ s}$) is presented. This corresponds, in the model hypothesis, to order of magnitude of the radiation levels estimated for the forward tracker region at the future LHC accelerator.

The increase of the initial oxygen concentration in silicon, from $2 \cdot 10^{15} \text{ cm}^{-3}$ to $4 \cdot 10^{17} \text{ cm}^{-3}$, conduces, after ten years of operation in the field characterised by a high and constant generation rate, to the increase of the concentrations of VO and C_iO_i centres, and to the decrease of the concentrations of V_2 , VP and C_iC_s ones. With the increase of oxygen concentration, a variation of the V_2O generation rate is observed, so that, from the studied cases, the maximum concentration for this defect is obtained for $5 \cdot 10^{16} \text{ cm}^{-3}$ initial oxygen. The increase of initial phosphorus is seen in the increase of concentration of VP centres, while the increase of initial carbon concentration has important consequences on the concentrations of C_iC_s centres. It is interesting to observe that in almost all cases, an equilibrium is reached between generation and annealing, and a plateau is obtained in the time dependence of the concentrations. The slowest is, in this respect, V_2O , that has the highest binding energy.

As underlined above, vacancy-oxygen formation in oxygen enriched silicon is favoured in respect to the generation of V_2 , V_2O and VP . This is an important feature that could be used for detector applications, determining the decrease of the leakage current [29]. At high oxygen concentrations, the concentration of VO centres attains a plateau during the 10 years period considered.

The other extreme situation corresponds to a generation rate $G_R = 200 \text{ VI} - \text{pairs}/\text{cm}^3 \text{ s}$, equivalent with a rate of defect production by protons from the cosmic ray spectra in the orbit near the Earth, at about 400 km, as will be the position of the International Space Station. The same concentrations of P , O and C have been considered as pre-existent in silicon as in Figure 4. For this generation rate, the increase of the oxygen concentration produces the decrease of the concentration of all centres, with the exception of the VO concentration, that, at these rates, it is not influenced by the oxygen content, and of the C_iO_i concentration, where an increase is observed.. As could be seen from Figure 5, as a consequence of the small rate of generation rate of vacancy - interstitial pairs, after ten years of operation the equilibrium between generation and annealing is not reached, the concentrations of defects being, with the exception of VP (that has a relatively low binding energy), slightly increasing functions of time.

All curves have been calculated for $20^{\circ}C$ temperature. Thermal generation has been taken into account in both cases, although it is important only for the silicon exposed to low rates of defect production.

The influence of the generation rate of primary defects on the concentration of stable defects and on their time evolution has also been investigated. In Figure 6 a) – f), the time evolution of the VO , VP , V_2 , V_2O , C_iO_i and C_iC_s concentrations is presented for six decades of generation rates of defects ($G_R = 7 \cdot 10^5 \div 7 \cdot 10^{10}$ $VI - pairs/cm^3s$), for silicon containing the following concentrations of impurities: 10^{14} P/cm^3 , 10^{16} O/cm^3 , 3×10^{15} C/cm^3 , at $20^{\circ}C$ temperature. At small times, the curves corresponding to different generation rates are all parallel and equidistant in a log-log representation. Starting from the highest generation rates, they start to increase slower (V_2 , VP), attain a plateau (V_2O), or even start to decrease (VO , C_iO_i , C_iC_s). The maximum attained can be the same, independent on the generation rate as is the case of VO concentration, or could be generation dependent (C_iC_s , C_iC_s).

The temperature is another important factor determining the time evolution of defects. In Figure 7 a) – f) and 6 a) – f), the effect of the temperature is studied for the same generation rates of primary defects as in Figure 4 and 5 respectively, for five temperatures: $+20^{\circ}C$, $+10^{\circ}C$, $0^{\circ}C$, $-10^{\circ}C$ and $-20^{\circ}C$. The concentrations of pre-existing impurities in silicon are as follows: 10^{14} cm^{-3} P , 10^{16} cm^{-3} O and 3×10^{15} cm^{-3} C . The decrease of the temperature decreases the generation rate of stable defects, with the exception of VP . Where the highest values correspond to the lowest temperature. The maximum values of the VO concentration are temperature independent; the values of the concentration on the plateau decrease with the decrease of temperature for C_iO_i and C_iC_s and increase for V_2O .

For silicon exposed to low rates of defect production the same amount of time (Figure 8), the process of defect production is slowed down. The most unexpected time dependence is for V_2 , that has the highest values at the lowest temperature.

In a previous paper [29], we demonstrated in concrete cases the importance of the sequence of irradiation processes, considering that the same total fluence can be attained in different situations: the ideal case of instantaneous irradiation, irradiation in a single pulse followed by relaxation, and respectively continuous irradiation process. As expected, after instantaneous irradiation the concentrations of defects are higher in respect with “gradual” irradiation.

After this analysis, the specific importance of the irradiation and annealing history (initial material parameters, type of irradiation particles, energetic source spectra, flux, irradiation temperature, measurement temperature, temperature and time between irradiation and measurement) on defect evolution must be to underline.

5.2 Correlation with detector parameters

a. The leakage current

It is well known that the dark current in a $p-n$ junction is composed by three different terms: the diffusion current, caused by the diffusion of the minority charge carriers inside the depleted region; the generation current, created by the presence of lattice defects inside the bulk of the detector; and surface and perimetral currents, dependent on the environmental conditions of the surface and the perimeter of the diode. The appearance of the defects after irradiation corresponds therefore in an increase of the leakage current of the detector by its generational term.

Inside the depleted zone, $n, p \ll n_i$ (n_i is the intrinsic free carrier concentration), each defect with a bulk concentration N_T causes a generation current per unit of volume of the form [34]:

$$I = qU = q\langle v_t \rangle n_i \frac{\sigma_n \sigma_p N_T}{\sigma_n \gamma_n e^{(E_i - E_i)/kT} + \sigma_p \gamma_p e^{(E_i - E_i)/kT}} \quad (19)$$

where γ_n and γ_p are degeneration factors, σ_n (σ_p) are the cross sections for majority (minority) carriers of the trap, $E_i = (E_c - E_v)/2$ and $\langle v_t \rangle$ is the average between electron and hole thermal velocities.

In the case of E and A centres and V_2^- and V_2^{--} defects, the current concentration can be expressed in the simple form:

$$I = q\langle v_t \rangle n_i \frac{\sigma_n}{\sigma_p} N_T e^{(E_i - E_i)/kT} \quad (20)$$

The primary effect in the recombination process is the change the charge state of the defect. The different charge states of the same deep centre may have different barriers for migration or for reacting with other centres. Thus, carrier capture can either enhance or retard defect migration or particular defect reactions. As a characteristics for detectors (as diode junction), the defect kinetics is dependent to the reverse - bias voltage during the irradiation [35].

The comparison between theoretical and experimental generation current densities after irradiation shows a general accord between experiment and the model results for the lepton irradiation and large discrepancies for the hadron case.

There could be several reasons for the observed discrepancies.

The model hypothesis of defects distributed randomly in semiconductors exclude the possibility of cluster defects. For this case, other mechanisms of defect formation are necessary, which suppose different reaction rates and correlation between the constituent defects of the cluster.

In the Shockley-Read-Hall model used currently for the calculation of the reverse current, each defect has one level in the gap, and the defect levels are uncoupled, thus the current is simply the sum of the contributions of different defects. In fact, the defects could have more levels, and charge states, as is the case of the divacancy, and also could be coupled, as in the case of clusters. As shown in the literature [36, 37], both cases can produces modifications of the generation rate.

Also the multivacancy oxygen defects as, e.g. V_3O , V_2O_2 , V_3O_2 , V_3O_3 , are not considered.

A model estimation of the time dependence of the leakage current, in conditions of continuous irradiations with pions of 200 MeV kinetic energy, in the conditions of the LHC [38, 39] and at 293K is presented in Figure 9, for two concentrations of oxygen in silicon: $5 \cdot 10^{16} \text{ cm}^{-3}$ and 10^{18} cm^{-3} , respectively. As underlined before, oxygen incorporation in silicon has beneficial effects, decreasing the reverse current. This conclusion is valid in the hypothesis of random distribution of defects inside the depleted zone of the p-n junction. These values are probably underestimated.

b. Effective doping concentration N_{eff} and charge collection efficiency

Currently, in the solid state physics, a standard procedure is used to determine the effective doping concentration. The determination of N_{eff} , or equivalently V_{dep} is performed by measuring the $C - V$ characteristics of the irradiated device, as:

$$C(V) = \frac{\epsilon A}{W(V)} = \sqrt{\frac{\epsilon N_{eff}}{2V_{dep}}} A \quad (21)$$

where A and W are the detector active area and depletion depth respectively. In heavily irradiated detectors, the strong dependence of the measured capacitance both on the temperature and the frequency of the a. c. test signal is observed and consequently frequency-dependent $C - V$ effect appear, $C(\omega, V)$.

This effect is usually modelled in literature by using one defect level with one charge state responsible for this phenomena. This is unrealistically and more detailed calculations are necessary. Zheng Li [40] elaborated a complex model including modelling the electrical neutral bulk and the space charge region for more acceptor-like trap levels but currently it is not used in the concrete calculations.

Conclusions

My personal conclusions can be summarised as:

After about 45 years of study of production and evolution of radiation induced defects in semiconductors, the field is now very broad, is summarised in books and represents the object of many conferences.

Fundamental progress has been obtained in the understanding of the phenomena of radiation induced damage in semiconductors, but more efforts are still necessary to clarify all the problems.

It is clear that the technological potential of semiconductor materials has not been exhaustively used and thus, there will continue to be new applications to be given and that will continue to reveal new problems and surprises.

Fundamental research is still necessary: both theoretical and in the experimental developments. Most probably, some of the empirical conclusions, never tested and confirmed, but included in the "folklore" of the field, are incorrect and must be eliminated.

Because the complexities of the problems, multidisciplinary studies and more efforts are necessary.

References

- [1] I. Lazanu, S. Lazanu, E. Borchini, M. Bruzzi, Nucl. Instr. and Meth. in Phys. Res. A 406 (1998) 259.
- [2] J.Hufner, Phys. Rep. 21C, no.1 (1975).
- [3] J.M.Eisenberg and D.S.Koltun, "Theory of Meson Interactions with Nuclei", J.Wiley & Sons, N.Y.1980.
- [4] F.Nichitiu, "Phase Shift Analysis in the Physics of Nuclear Interactions", Editura Academiei RSR 1980 (in romanian).
- [5] G.D.Harp, K.Chen, G.Friedlander, Z.Frankel, and J.M.Miller, Phys.Rev. C8 (1973) 581.

- [6] D.Ashery and J.P.Schiffer, *Ann.Rev.Nucl.Part.Sci.* 36 (1986) 207.
- [7] V.S.Barashenkov, Preprint JINR Dubna P2-90-158 (1990) (in russian).
- [8] V.S.Barashenkov, V.A.Polansky, and A.N.Sosnin, Preprint JINR Dubna P2-90-159 (1990) (in russian).
- [9] D.Ashery, I.Navon, G.Azuelos, H.K.Walter, H.J.Pfeiffer, and F.W.Schleputz, *Phys.Rev.* 23 (1981) 2173.
- [10] A.Mihul, T.Angelscu, R.Ionica, Yu.A.Shcherbakov, I.Lazanu, T.Preda, and R.Garfanini, *Nuovo Cimento* 105A (1992) 1637.
- [11] A.Altman, D.Ashery, E.Piasetzky, J.Lichtenstadt, A.I.Yavin, W.Berti, I.Felawa, H.K.Walter, R.J.Powers, R.G.Winter, and J.v.d.Pluym, *Phys.Rev.* C34 (1986) 1757.
- [12] S. M. Levenson et al., *Phys. Rev. Lett* 47 (1981) 479.
- [13] C.L.Morris, R.D.ransome, B.G.Ritchie, Z.D.Zumbro, D.L.Watson, C.Fred Moore, *Proc. Int.. Workshop on Pions in Nuclei, Spain 1991*, eds. E.Oset, M.J.Vincente Vacas, C.Garcia Recio, p. 495.
- [14] P.Weber, J.Mc.Alistair, R.Osszewski, A.Feltham, M.Hanna, D.Humphrey, R.R.Johnson, G.J.Lolos, Z.Papandreou, M.Pavan, C.Ponting, M.Rozon, M.Sevior, G.R.Smith, V.Sossi, R.Tacik, and D.Vetterli, *Proc. Int. Workshop on Pions in Nuclei, Spain 1991*, eds. E.Oset, M.J.Vincente Vacas, C.Garcia Recio, p. 479.
- [15] G. H. Kinchin, R. S. Pease, *Report on Progress in Physics* 18 (1955) 1.
- [16] J. Lindhard, V. Nielsen, M. Schraff, P.V. Thomsen, *Mat. Phys. Medd. Dan. Vid. Sesk.* 33 (1963) 1.
- [17] S. Lazanu, I. Lazanu, *Nucl. Instr. Meth.Phys. Res. A* **462** :530 (2001).
- [18] A. Chilingarov, D. Lipka, J. Meyer, T. Sloan, *Nucl. Instr. Meth.Phys. Res. A* **449** (2000) 277.
- [19] S.Lazanu and I.Lazanu, *Nucl. Instr. Meth. Phys. Res. A* 419 (1998) 570.
- [20]. G. P Summers, E. A. Burke, Ph. Shapiro, S. R. Messenger, R. J. Walters *R. IEEE Trans. Nuclear Science*, **NS 40**, :1372 (1993).
- [21] A. Van Ginneken, Preprint Fermi National Accelerator Laboratory, **FN-522**, 1989
- [22] A. M. Ougouag, J. G. Williams, M. B. Danjaji, S.-Y. Yang, S.-Y., *IEEE Trans. Nuclear Science*, **NS -37**, 2219 (1990).
- [23] J. Bourgoin, and M. Lannoo, " Point Defects in Semiconductors", (edited by M. Cardona, P. Fulde, H. J. Quisser), (Springer Verlag, Berlin, 1983) Springer Series in Solid State Sciences, vol. 35.
- [24] M. Bruzzi, *IEEE Trans. Nucl. Sci*, **NS-48** (2001) 960.
- [25] M. Moll, E. Fretwurst, G. Lindstrom, *Nucl. Instrum. Meth. Phys. Res. A* **439** (2000) 282.
- [26] B. C. Mac Evoy, A. Santacchia, G. Hall, *Physica* **B 273-274** (1999) 1054.
- [27] Y. H. Lee and J. W. Corbett, *Phys. Rev.* **B 13**: (1976) 2653.
- [28] S. Lazanu, I. Lazanu, *Nucl. Instr. Meth. Phys. Res. B* **183** (2001) 383.
- [29] I. Lazanu, S. Lazanu, "Radiation defects in silicon due to hadrons and leptons, their annealing and influence on detector performance", in press to *Physica Scripta*.
- [30] Z. Su, A. Husain,, J. W. Farmer, *J. Appl. Phys.* 67 (1990) 1903
- [31] S.D.Brotherton and P. Bradley, *J. Appl. Phys.* 53 (1982) 5720
- [32] L. W. Song, B. W. Benson, G. D. Watkins, *Phys. Rev.* **B 33** (1986) 1452.
- [33] U. Biggeri, E. Borch, M. Bruzzi, Z. Li, S. Lazanu, *IEEE Trans. Nucl. Sci.* **NS 41**, 964 (1994).
- [34] E. Borch, M. Bruzzi, M. S. Mazzoni, *Nucl. Instrum. Meth. Phys. Res. A* **310**, 273 (1991).
- [35] T. S. Pantelides, editor "Deep Centers in Semiconductors", Gordon & Breach Science Publishers, Second Edition, 1992, p.65
- [36] G. Lutz, *Nucl. Instrum. Meth. Phys. Res. A* **377**, 324 (1996).
- [37] S. C. Choo, *Phys. Rev.* **B 1**, 687 (1970).
- [38] P. A. Aarnio, M. Huhtinen, *Nucl. Instr. Meth. Phys. Res. A* **336**, 98 (1993).
- [39] CMS Collaboration, CMS Technical Proposal, CERN/LHCC 94-38, 1994
- [40] Z. Li, *Nucl. Instr. Meth. Phys. Res. A* 342 (1994) 105.

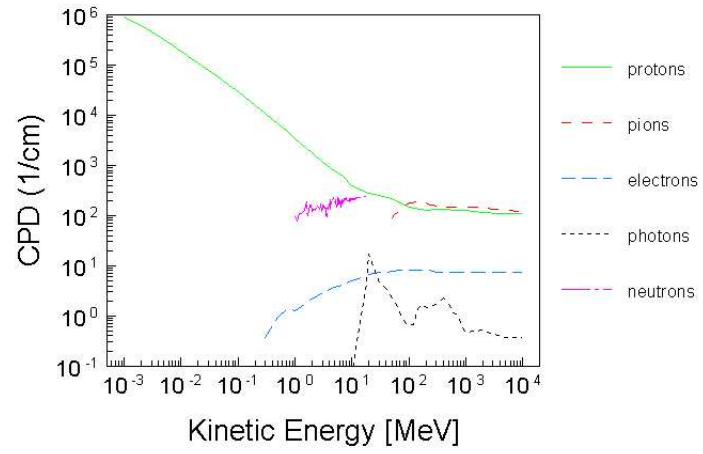


Figure 1
Energy dependence of the concentration of primary defects on unit fluence induced
by protons, pions, electrons, photons and neutrons in silicon

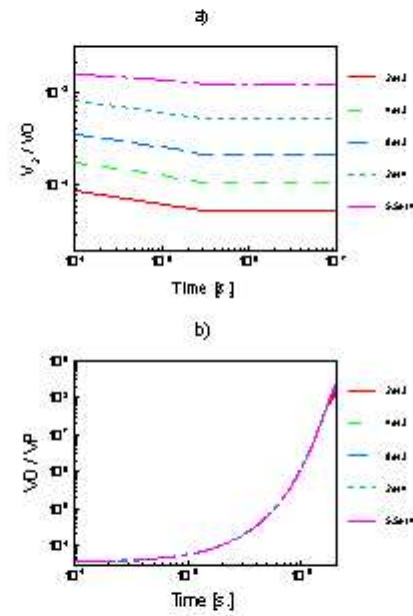


Figure 2

Time dependence for a) V_2/VO and b) VO/VP concentrations calculated for silicon with $1.4 \cdot 10^{14} P/cm^3$, $5 \cdot 10^{17} O/cm^3$, and $3 \cdot 10^{15} C/cm^3$, by 12 MeV electron irradiation, with the flux $5.8 \cdot 10^{10} e/cm^2 s$, up to the fluences: $2 \cdot 10^{13} e/cm^2$, $4 \cdot 10^{13} e/cm^2$, $8 \cdot 10^{13} e/cm^2$, $2 \cdot 10^{14} e/cm^2$ and $5.5 \cdot 10^{13} e/cm^2$, followed by relaxation (see reference [31]).

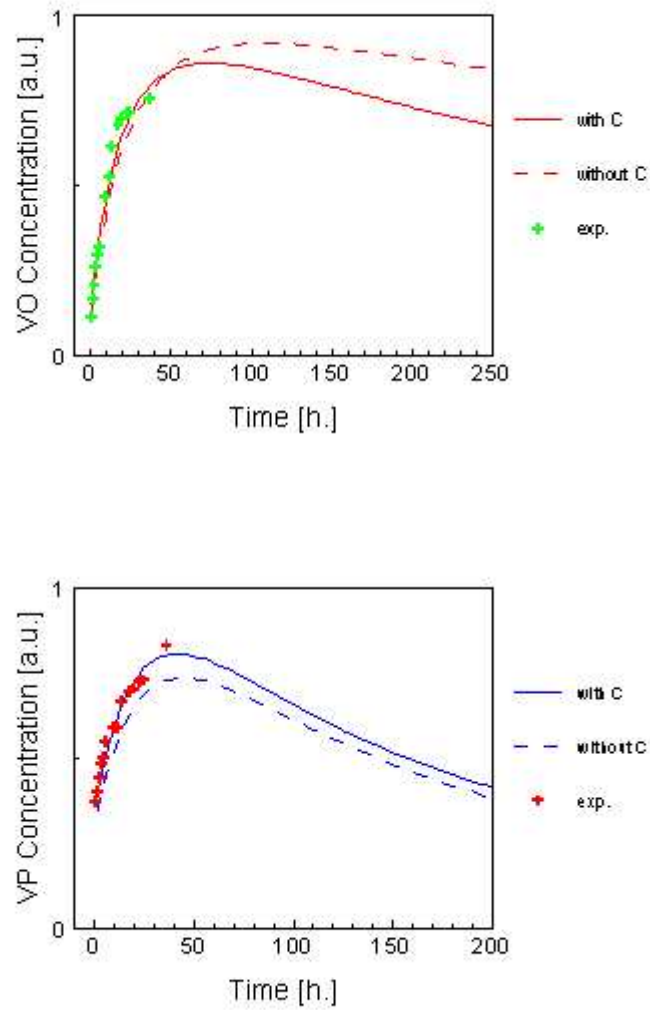


Figure 3

Time dependence of VO and VP concentrations after electron irradiation: crosses - experimental data from reference [31]; continuous line present model calculations; dashed line - without the consideration of carbon contribution to defect formation.

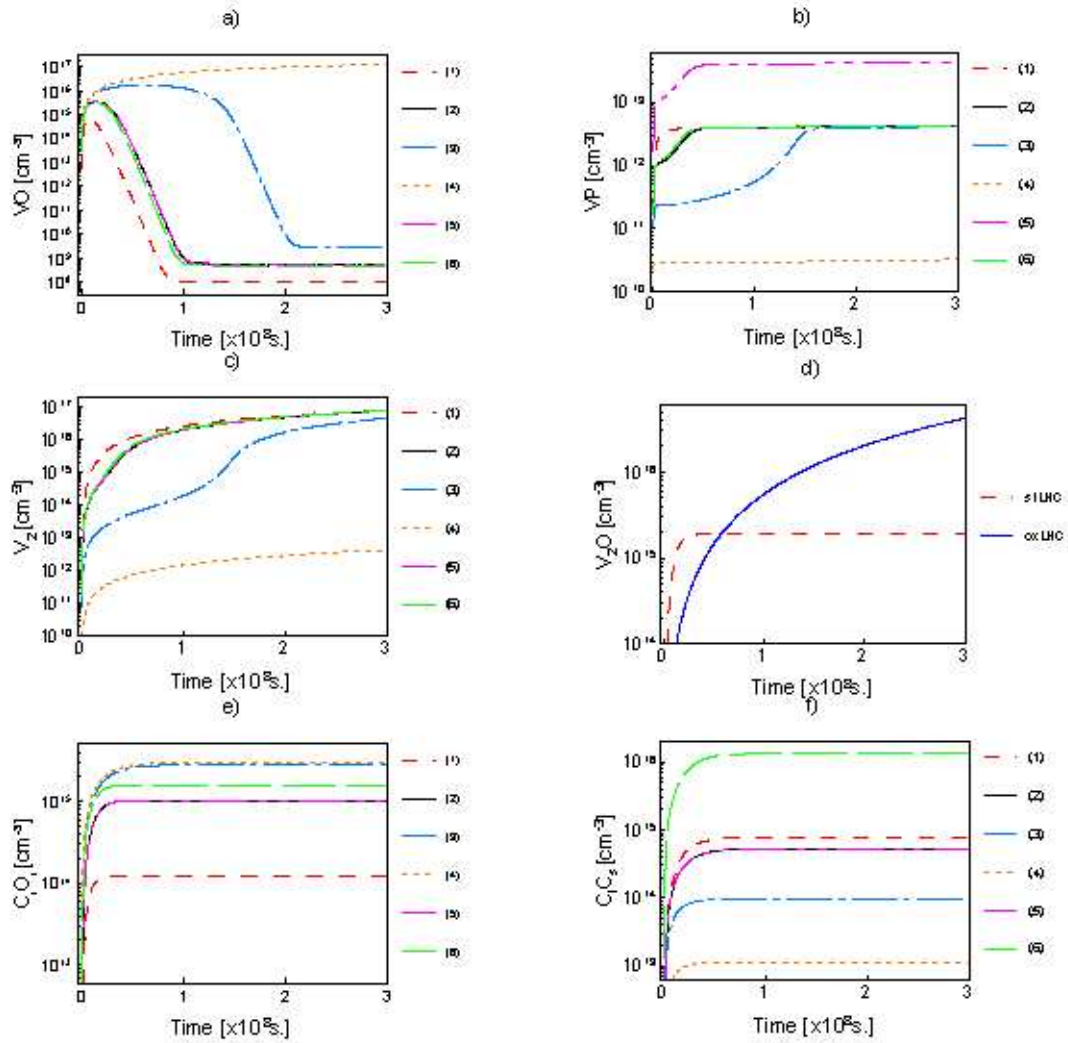


Figure 4

Time dependence of the concentrations of a) VO , b) VP , c) V_2 , d) V_2O , e) C_iO_i and f) C_iC_s induced in silicon with the following concentrations of impurities: (1): $10^{14} P/cm^3$, $2 \cdot 10^{15} O/cm^3$, and $3 \cdot 10^{15} C/cm^3$;

(2): $10^{14} P/cm^3$, $10^{16} O/cm^3$ and $3 \cdot 10^{15} C/cm^3$; (3): $10^{14} P/cm^3$, $5 \cdot 10^{16} O/cm^3$, and

$3 \cdot 10^{15} C/cm^3$; (4): $10^{14} P/cm^3$, $4 \cdot 10^{17} O/cm^3$, and $3 \cdot 10^{15} C/cm^3$; (5): $10^{15} P/cm^3$, $10^{16} O/cm^3$,

and $3 \cdot 10^{15} C/cm^3$; (6): $10^{14} P/cm^3$, $10^{16} O/cm^3$, and $3 \cdot 10^{16} C/cm^3$ by a generation rate

$$G_R = 7 \cdot 10^8 \text{ VI pairs/cm}^3 \text{ s, at } 20^0 \text{ C.}$$

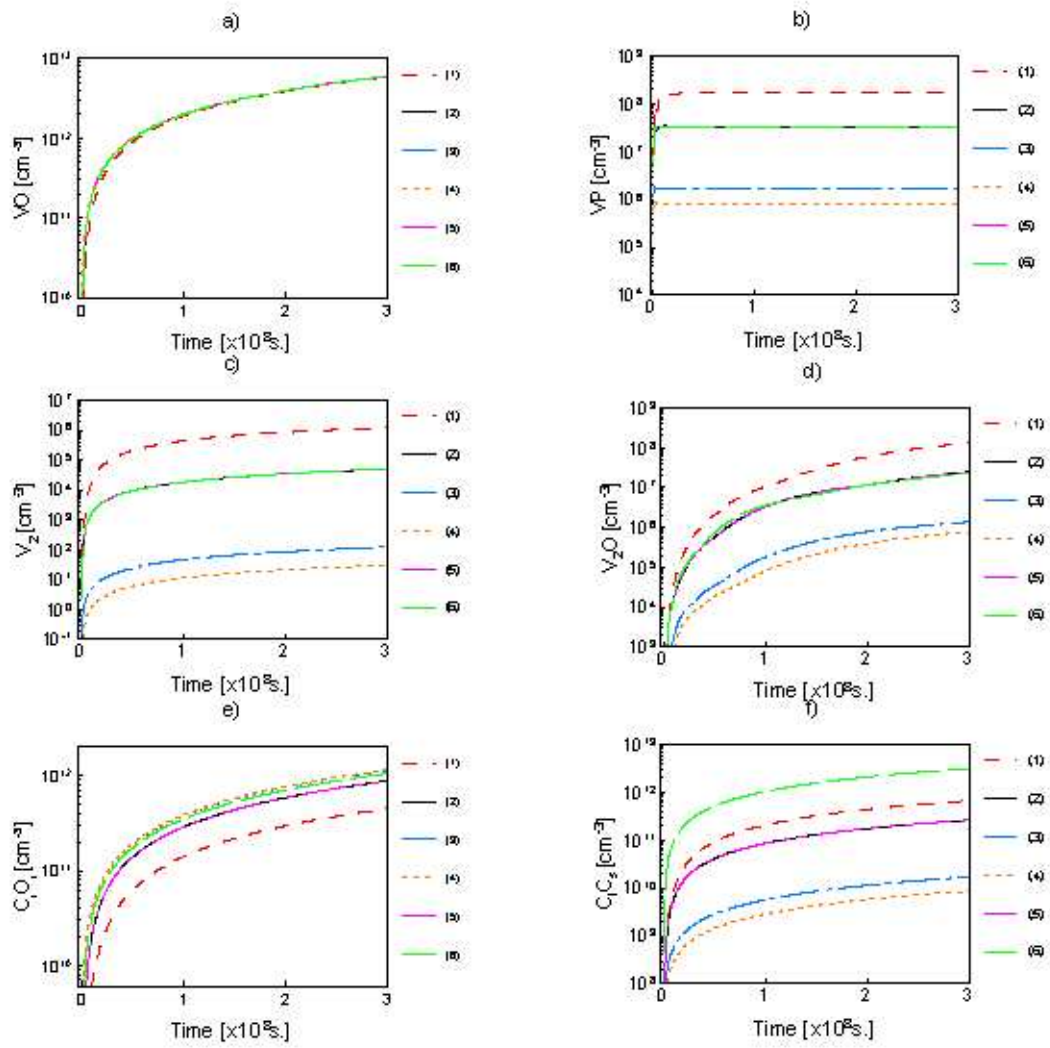


Figure 5

Same as Figure 4, $G_R = 200$ VI pairs/cm³ s.

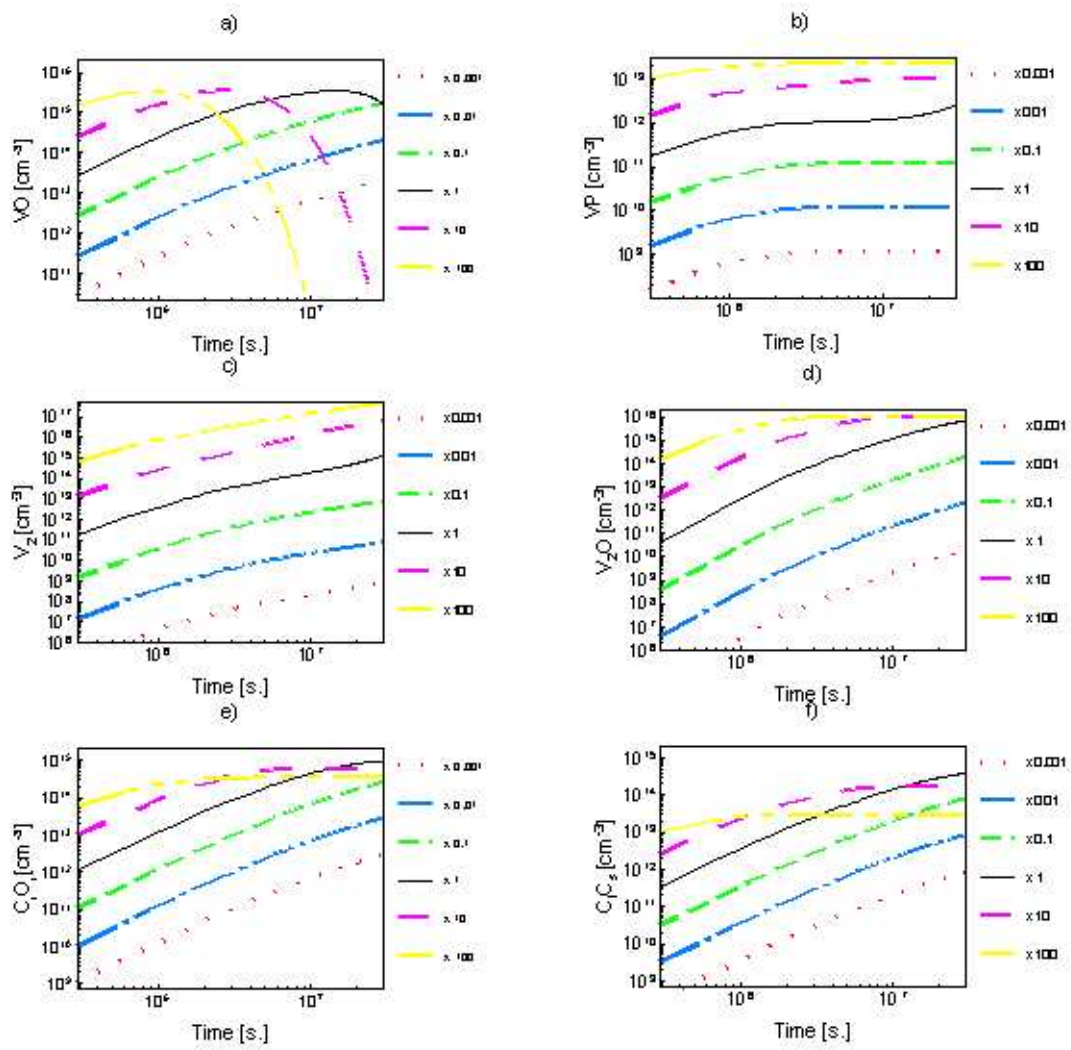


Figure 6

Time dependence of the concentrations of a) VO , b) VP , c) V_2 , d) V_2O , e) C_iO_i and f) C_iC_s induced in silicon with: $10^{14} P/cm^3$, $10^{16} O/cm^3$, $3 \cdot 10^{15} C/cm^3$, by continuous irradiation

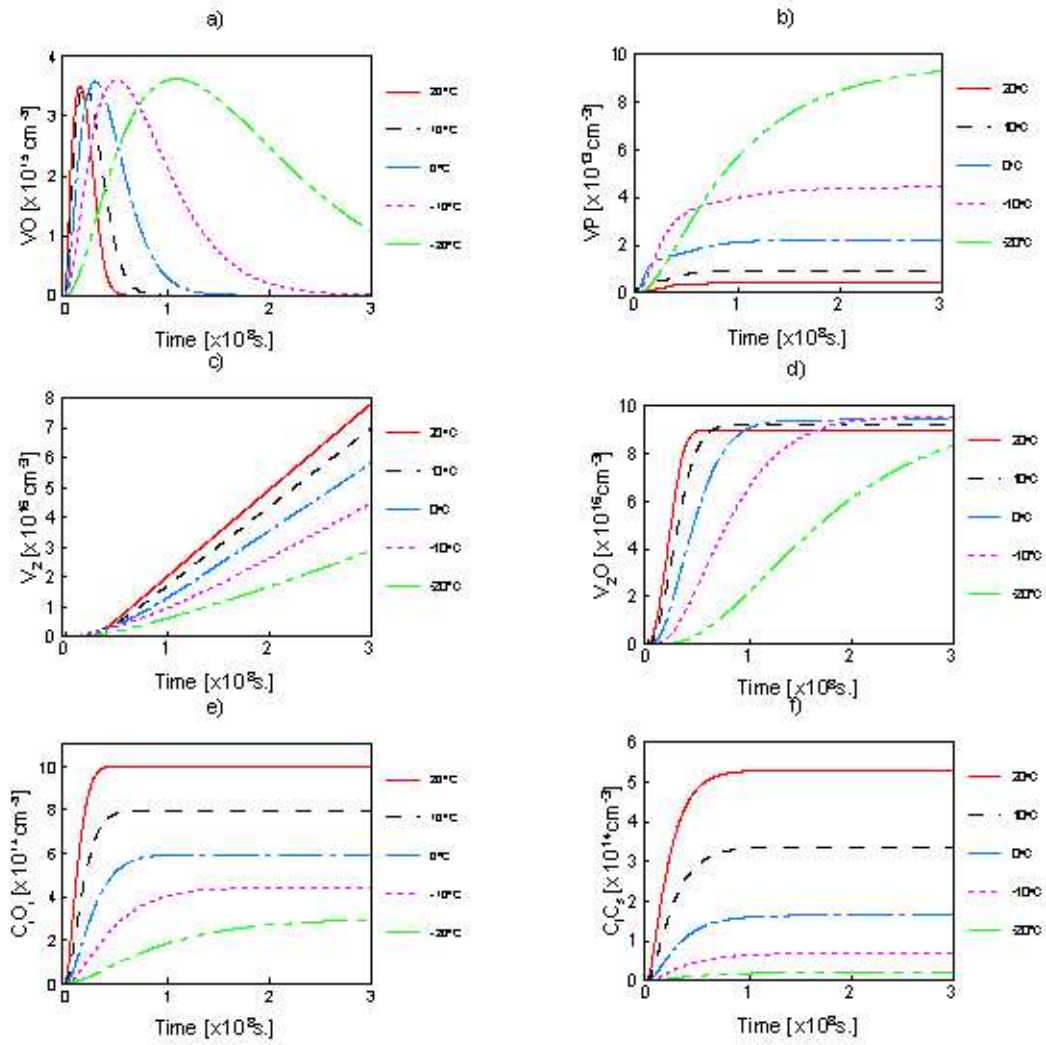


Figure 7

Time dependence of the concentrations of a) VO , b) VP , c) V_2 , d) V_2O , e) C_iO_i and f) C_iC_s induced in silicon with: $10^{14} P/cm^3$, $10^{16} O/cm^3$, and $3 \cdot 10^{15} C/cm^3$, by continuous irradiation in the same conditions as in Figure 4, at $20^\circ C$, $10^\circ C$, $0^\circ C$, $-10^\circ C$, and $-20^\circ C$.

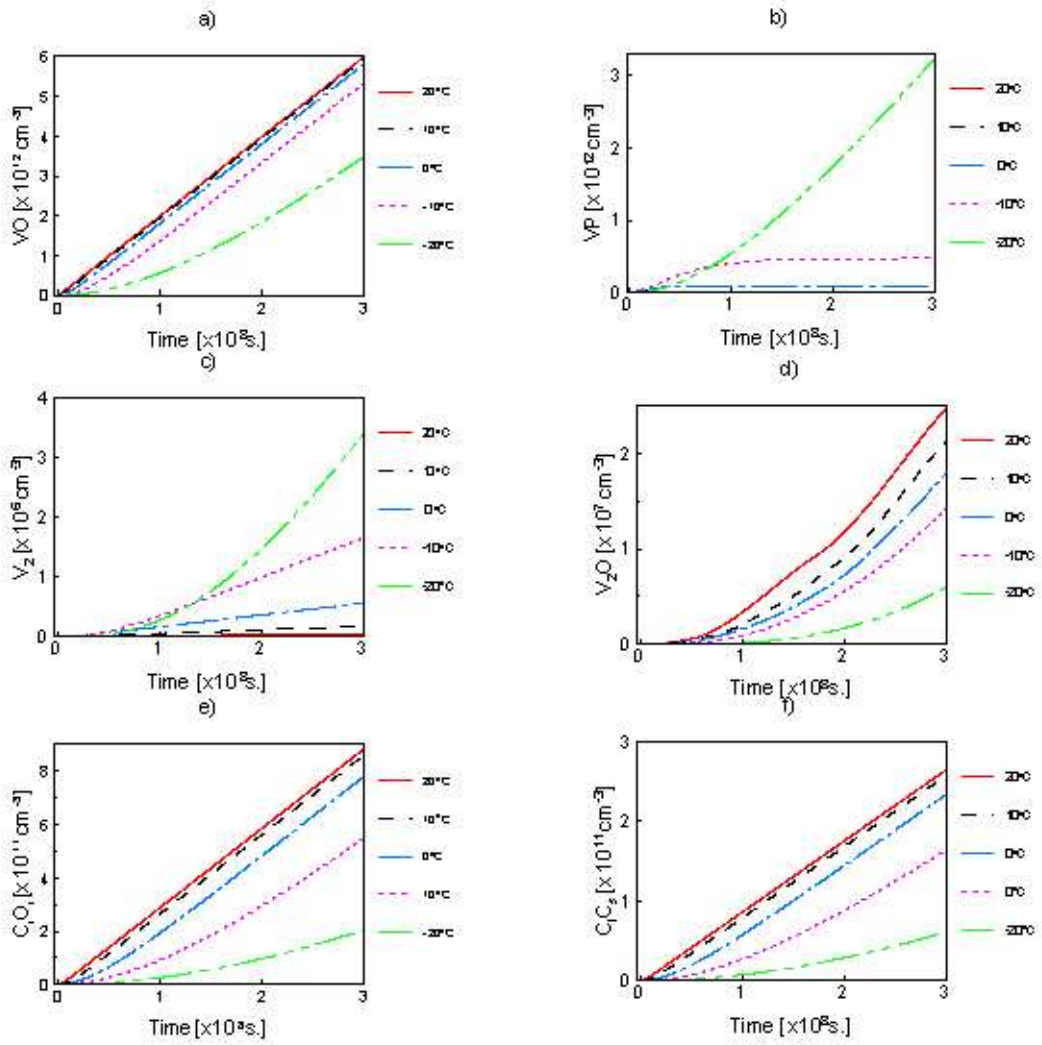


Figure 8

Time dependence of the concentrations of a) VO , b) VP , c) V_2 , d) V_2O , e) C_iO_i and f) C_iC_s induced in silicon with: $10^{14} P/\text{cm}^3$, $10^{16} O/\text{cm}^3$, and $3 \cdot 10^{15} C/\text{cm}^3$, by continuous irradiation in the same conditions as in Figure 5, at 20°C , 10°C , 0°C , -10°C , and -20°C .

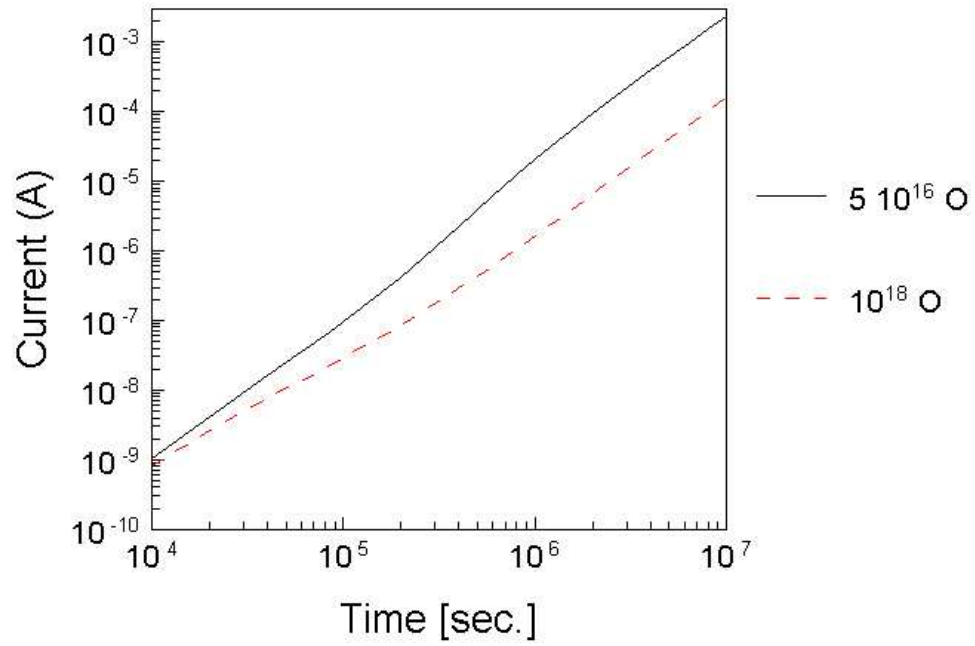


Figure 9

Time dependence of the leakage current, in conditions of continuous irradiations with pions of 200 MeV kinetic energy, in the conditions of the LHC, at 293K, for two concentrations of oxygen in silicon: $5 \cdot 10^{16} \text{ cm}^{-3}$ and 10^{18} cm^{-3} , respectively.